DOI:10.1021/jf903054e

JOURNAL OF AGRICULTURAL AND FOOD CHEMISTRY
ARTICLE

# Chemical Modeling of Heme-Induced Lipid Oxidation in Gastric Conditions and Inhibition by Dietary Polyphenols

Bénédicte Lorrain,[†] Olivier Dangles,[†] Claude Genot,[‡] and Claire Dufour*,[†]

[†]UMR408 Safety and Quality of Plant Products, INRA, University of Avignon, Avignon, France, and [‡]UR1268 Biopolymères Interactions Assemblages, INRA, Nantes, France

The gastric tract may be the first site exposed to diet-related oxidative stress. After food intake, dietary iron such as (met)myoglobin, the pigment of meat, oxygen, and polyunsaturated lipids come into close contact. The main goal of this work is the in vitro investigation of lipid oxidation taking place in the gastric compartment and its inhibition by dietary polyphenols. Oil-in-water emulsions stabilized either by bovine serum albumin (BSA) or egg yolk phospholipids (PL) were designed to model the gastric content. The metmyoglobin-initiated lipid oxidation led to the accumulation of lipid-derived conjugated dienes and volatile aldehydes. These reactions were faster in the BSA model than in the PL model, highlighting the influence of the interfacial composition. Quercetin, rutin, (+)-catechin, caffeic acid, and chlorogenic acid proved to be better inhibitors than α-tocopherol and ascorbic acid. Emulsions as models of the gastric environment are valuable tools to study the stability of macro- and micronutrients.

**KEYWORDS: Antioxidant; lipid oxidation; metmyoglobin; oil-in-water emulsion; polyphenol; gastric tract;**

## INTRODUCTION

Diets rich in fruits and vegetables, such as the Mediterranean diet, are associated with a lower incidence of cardiovascular diseases and possibly cancer (*1*). Among vegetable microconstituents, polyphenols are possible mediators of these beneficial effects (*2*). In this nutritional perspective, the bioavailability of dietary polyphenols comes up as a crucial step. After the ingestion of a meal rich in plant products, polyphenols are poorly absorbed from the gastrointestinal (GI) tract and undergo extensive metabolization before reaching the blood and lymphatic circulations. In plasma, they mainly circulate as sulfates and glucuronides of the aglycones and their catechol *O*-methylethers, mostly bound to serum albumin and in concentrations rarely exceeding 1 μM (*3*). Additionally, polyphenol conjugates may exhibit biological activities different from those of the native forms and are much less potent antioxidants (*3*, *4*).

By contrast, native forms of polyphenols are present in much larger concentrations in the GI tract, which has been proposed as a major site for diet-related oxidative stress and antioxidant activity (*5*). For instance, after food intake, dietary iron, oxygen, and emulsified lipids closely interact in the gastric compartment, and substantial lipid oxidation can take place (*6*, *7*). The lipid hydroperoxides thus formed may not reach the intestine but rather decompose in the stomach into hydroxy fatty acids and potentially toxic electrophiles such as aldehydes and epoxides (*8*−*10*), which can be incorporated into the gastric and intestinal tissues (*8*) before being delivered to the liver by chylomicrons and finally to the blood circulation within VLDL particles (*11*). Moreover, covalent binding of aldehydes to apolipoprotein is strongly implicated in the atherogenicity of LDL (*9*). Interestingly, increased concentrations of minimally modified LDL particles enriched in lipid oxidation products have been detected in the blood of volunteers who have ingested a high-fat diet (*12*). Such particles are likely precursors of highly oxidized LDL particles, which are taken up by macrophages in the subintimal space of arteries during the development of fatty streaks. Hence, it can be concluded that there is growing evidence for a link between dietary lipid oxidation products, either ingested with the diet or formed in the gastric compartment, and the risk of developing cardiovascular diseases (*9*, *10*).

The aim of the present study is to investigate the lipid oxidation initiated by metmyoglobin, one of the main forms of dietary iron, and its inhibition by dietary polyphenols and antioxidant vitamins. Mildly acidic sunflower oil-in-water emulsions, stabilized either by bovine serum albumin (BSA) or phospholipids (PL), were designed to model the gastric content. Triglycerides rather than free fatty acids (*7*, *13*−*15*) were used as the source of fat daily consumed in the western world (100−150 g of triglycerides and 2−10 g of phospholipids) (*6*). As to phenolic compounds, they are mainly provided through the consumption of fruits, vegetables, cereals, and corresponding processed products. For example, rutin (quercetin-3-*O*-rutinose) is largely found in apple and tomato skins, while several quercetin glycosides contribute to the polyphenol pool of onions. Caffeic acid derivatives are abundant in coffee and potato, while catechin oligomers (condensed tannins) are largely distributed in fruits and wine. Vitamin C (L-ascorbic acid) can be regarded as the ubiquitous hydrophilic antioxidant of fruits and vegetables, whereas the

*To whom correspondence should be addressed. UMR408, INRA, Site Agroparc, 84914 Avignon Cedex 9, France. Tel: + 33 432 72 25 15. Fax: + 33 432 72 24 92. E-mail: claire.dufour@avignon.inra.fr.

 Published on Web 11/13/2009 

lipophilic α-tocopherol reaches high concentrations in vegetable oils. Chemical mechanisms involved in metmyoglobin-initiated lipid oxidation and its inhibition by the above-cited antioxidants are discussed in both models.

## MATERIALS AND METHODS

**Materials.** Quercetin, rutin, caffeic acid, chlorogenic acid, (+)-catechin, 3,4-dihydroxybenzoic acid, (+)-α-tocopherol, L-ascorbic acid, 1-octen-3-ol, hexanal, pentanal, (*E*)-2-heptenal, (*E*)-2-octenal, bovine serum albumin (BSA) (fraction V A-9647, MW ca. 66500 g $mol^{-1}$), myoglobin (from horse heart, MW ca. 17600 g $mol^{-1}$), and L-α-phosphatidylcholine from egg yolk (PL, type X-E) were purchased from Sigma-Aldrich (Saint-Quentin Fallavier, France). Analysis of L-α-phosphatidylcholine (type X-E) was performed by HPLC coupled to an evaporative light scattering detector (DDL Sedex 55) on a Supelcosil TM LC-Si column (5 μm, 250 × 4.6 mm, Supelco). The solvent system was a gradient of A ($CHCl_3$) and B (MeOH/30 vol. % aqueous $NH_3$/$CHCl_3$ 460/35/5 v/v/v) with 0% B at 0 min, 20% B at 10 min, and 100% B between 20 and 30 min. Quantification was carried out from calibration curves with standards (L-α-phosphatidylethanolamine from egg yolk, type III, L-α-phosphatidylcholine (PC) from bovine brain, and sphingomyelin, from Sigma-Aldrich, Saint-Quentin Fallavier, France). Results indicated that L-α-phosphatidylcholine (type X-E) was composed of phosphatidylcholine (47 wt %), phosphatidylethanolamine (18%), sphingomyelin (4%), and lysophosphatidylcholine (4%) along with a neutral fraction (24%). The oxidation product (2-(3,4-dihydroxybenzoyl)-2,4,6-trihydroxybenzofuran-3-(*2H*)-one) was obtained by oxidation of quercetin in the presence of copper as described in ref *16*. All solvents (2-propanol, pentane, acetonitrile, dimethylsulfoxide, and methanol) were purchased from Fisher Scientific Bioblock (Illkirch Cedex, France) and were of analytical grade ( > 99.4%). A 5 mM phosphate buffer (pH 5.8), prepared with Millipore Q-100 Plus water, was passed through a column of CHELEX-100 chelating resin (Bio-Rad) to remove contaminating metal ion traces.

Commercial sunflower oil (Carrefour store) was stripped of tocopherols using adsorption chromatography on an alumina column (aluminum oxide 90 neutral activity, Merck) and pentane as eluting solvent (*17*). Pentane was removed in vacuo by rotary evaporation. Absence of α-tocopherol was confirmed by HPLC coupled to a UV−vis detector by comparison to an α-tocopherol standard. Stripped sunflower oil contained around 63% 18:2 $n-6$, 25% 18:1 $n-9$, 7% 16:0, and 5% 18:0 as major fatty acids (*17*). It was stored under $N_2$ at −20 °C.

**Preparation and Characterization of Gastric Model Emulsions.** Two different oil-in-water emulsions, stabilized either by BSA or by egg PL, were prepared to model the gastric content. In a 50 mL round-bottom flask, 1 g of stripped sunflower oil was added to 7.9 mL of either BSA (138 mg) or PL (208 mg) previously dispersed in 5 mM phosphate buffer at pH 5.8. The PL dispersion was best achieved using a rotor stator homogenizer (UltraTurrax T25, IKA) at 24000 rpm for 1.5 min twice. The oil and aqueous phases were then homogenized at 24000 rpm for 2 min. The coarse emulsion was swept with $N_2$ for 5 min before probe sonication for 2 periods of 30 s with a rest interval of 30 s for the BSA-stabilized emulsions or 6 periods of 30 s with intervals of 30 s in ice for the PL-stabilized emulsions (130 W, 20 kHz, Bioblock Vibracell). The final pH for the BSA model was close to 6.0.

A volume of 0.1 mL of the antioxidant in acetonitrile/DMSO (4:1, v/v) was added via syringe to ensure final concentrations in the range 0−100 μM. Ascorbic acid was dissolved in water. Then, lipid oxidation was initiated by adding 1 mL of a 200 μM solution of metmyoglobin ($\varepsilon$ = 7700 $M^{-1}$ $cm^{-1}$ at 525 nm (*18*)) in the buffer to a final concentration of 20 μM. The system was protected by punched parafilm before being placed in an oven at 37 °C under constant magnetic stirring.

The size distribution of the lipid droplets was determined in triplicate with a laser particle size analyzer (Mastersizer 2000, Malvern Instruments, Orsay, France). Calculations were performed using the Mie theory with the following refractive indexes: 1.475 for oil, 1.333 for the dispersant, and an absorbance value of 0.01 for the emulsion particle. The mean diameter was reported as the surface-weighted diameter $d_{32}$.

**Measurement of Conjugated Dienes Issued from Lipid Oxidation.** Every hour, 200 μL of emulsion were diluted by a factor 20 in 2-propanol. BSA was removed by centrifugation (4 min at 5600 rpm, 5 °C). After dilution of the supernatant by a factor 10 or 20, the concentration of conjugated dienes (CD) was determined by measuring the absorbance at 233 nm (HP 8453 diode-array spectrometer equipped with a magnetically stirred cell; optical path length = 1 cm) and by using 27000 $M^{-1}$ $cm^{-1}$ as the molar absorption coefficient for conjugated linoleyl hydroperoxides (*19*). All analyses were run in duplicate except for antioxidant concentrations equal to 100 μM (triplicate). Control experiments without antioxidant were repeated at least 4 times. For the controls and 100 μM antioxidant concentrations, the area under the CD concentration versus time curve (AUC) was integrated by a polyhedral method. The antioxidant capacity was expressed as the relative AUC: (100 × AUC for 100 μM antioxidant)/control AUC.

**Measurement of Volatile Compounds Issued from Lipid Oxidation.** Hexanal, pentanal, 1-octen-3-ol, (*E*)-2-heptenal, and (*E*)-2-octenal were analyzed by gas chromatography after sampling of the volatiles in the headspace of the emulsions with solid-phase microextraction (*17*). The SPME fiber, coated with carboxen/polydimethylsiloxane (length = 10 mm; thickness = 75 μm; Supelco), was left to exposure in the headspace for 10 min at 37 °C before being transferred to the injection port of a GC-MS (GC QP 20120, Shimadzu) equipped with a 0.75 mm i.d. linear set at 250 °C for a 3 min desorption with a split ratio of 15. Helium at a 35 cm $s^{-1}$ velocity was used as the carrier gas. Volatiles were separated on a Varian CP-Sil 8 CB fused silica capillary column (30 m × 0.25 mm, 0.5 μm). The temperature program was as follows: 40 °C during 2 min, then 10 °C $min^{-1}$ until 240 °C. The mass spectrometer was operated in the electron impact (EI) mode at 70 eV in the $m/z$ range 29−250 at a speed of 2 scans $s^{-1}$. The temperatures of the ion source and of the transfer line were 200 and 240 °C, respectively. Detected compounds were identified by matching spectra against the NIST library (v.2.0).

Concentrations measured in the headspace were used to calculate concentrations in solution through a calibration step. For this, the 5 selected volatile compounds were dissolved in the tocopherol-stripped sunflower oil at concentrations of 960 mg/kg oil for hexanal, 110 mg/kg for pentanal, 240 mg/kg for (*E*)-2-heptenal, 340 mg/kg for 1-octen-3-ol, and 27 mg/kg for (*E*)-2-octenal, in closed vials with limited headspace volume. This flavored oil was then diluted by the tocopherol-stripped sunflower oil (1/10, 1/50, 1/100, and 1/250). The corresponding five BSA- or PL-stabilized emulsions were prepared following the two-step emulsification procedure described above. After 45 min of equilibrium at 37 °C, SPME-GC/MS analysis was performed for each emulsion leading to calibration curves of GC peak areas versus volatile concentrations in the emulsions.

**Structural Modification of BSA during Lipid Oxidation.** Front-face fluorescence spectra were obtained with a 3D spectrofluorometer (Hitachi F-4500) equipped with a solid sample holder for front-face measurement at 20 °C ± 2 °C) (*20*). The excitation and emission slit widths were set at 5 nm. The emulsion was placed in a 26 μL quartz cell (optical path length = 0.1 mm). Emission spectra of tryptophan residues were recorded from 300 to 450 nm after excitation set at 290 nm. Formation of new fluorescent pigments was best detected with excitation set at 360 nm, while emission was collected from 365 to 550 nm. All spectra were acquired in triplicate.

**Quantitative and Qualitative Analyses of Polyphenols and Their Oxidation Products.** A 200 μL emulsion aliquot was diluted by a factor 3 in 2-propanol and centrifuged at 10000 rpm for 2 min. The supernatant was frozen at −25 °C until HPLC analysis. HPLC-MS analyses were carried out on a Hewlett-Packard 1050 apparatus coupled to a UV−visible diode-array detector and a Micromass platform LCZ 4000 mass spectrometer. Mass analyses were performed in the negative electrospray ionization mode with cone voltages of 25 and 50 V and a desolvation temperature of 250 °C. Separation was obtained at 35 °C using an Alltima C18 column (5 μm, 150 mm × 4.6 mm) and a guard column (7.5 mm × 4.6 mm). The solvent system was a gradient of A (0.05% aqueous $HCO_2H$) and B (MeCN) at a flow rate of 1 mL $min^{-1}$. Initial B was set at 5%. For quercetin: 60% B at 15 min and 100% B at 20 min. For rutin: 35% B at 15 min and 100% B at 25 min. For (+)-catechin: 60% B at 20 min and 100% B at 25 min. For caffeic acid: 100% B at 30 min. For chlorogenic acid: 20% B at 15 min and 100% B at 25 min. Isocratic solvents were used for α-tocopherol (MeOH) and ascorbic acid (5% MeOH in 0.05% aq. $HCO_2H$). Quercetin and rutin were detected at 365 nm, chlorogenic and caffeic acids at 330 nm, catechin and all new products at 280 nm, α-tocopherol at 293 nm, and ascorbic acid at 254 nm. Authentic standards were used for calibration curves.

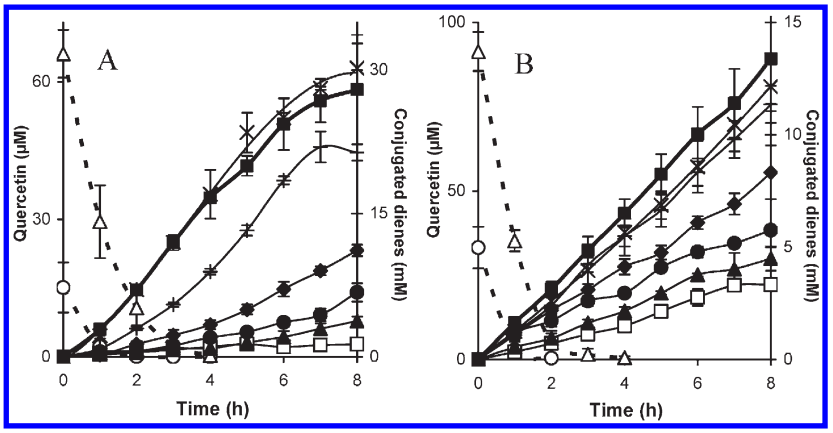


**Figure 1.** Inhibition by quercetin of the accumulation of conjugated dienes in the BSA model (**A**) and in the PL model (**B**) in the presence of metmyoglobin (20 $\mu$M). Quercetin concentrations: 0 (control, ■), 5 (×), 10 (+), 25 (♦), 50 (●), and 100 $\mu$M (▲). Concomitant oxidation of quercetin at 50 $\mu$M (○) and 100 $\mu$M (△). Control in the absence of metmyoglobin (□).

**Phenol-BSA Binding.** BSA was daily dissolved in the 5 mM phosphate buffer at pH 5.8. Steady-state fluorescence was recorded on a thermostatted Xenius spectrofluorometer (SAFAS). All studies were performed at 25 ± 1 °C using 10 nm excitation and emission slit widths. To 2 mL of 75 $\mu$M BSA placed in a quartz cell (length = 1 cm) were added 3 to 20 $\mu$L aliquots of quercetin (7.5 mM) or rutin (22 mM) solutions in MeOH. Excitation was set at 450 nm and emission fluorescence collected at 530 nm. Each experiment was performed in triplicate. Fluorescence of unbound phenols was negligible. The absorbance of unbound phenols at the excitation wavelength remained below 0.2, thus limiting the inner filter effect. A Scatchard analysis was first performed assuming $n$ identical binding sites for albumin. Optimized values for the binding constant ($K_1$), the molar fluorescence intensity of the complex ($f_1$), and the stoichiometric coefficient ($n$) were estimated by fitting the $F$ versus $Lt$ curves against eqs 1 and 2 using a nonlinear least-squares regression program (Scientist from MicroMath, Salt Lake City, USA) where $F$ is the fluorescence intensity, [$L$] the free ligand concentration, $L_t$ the total ligand concentration, and $c$ the total albumin concentration (*21*).

$$F = f_1 c \frac{nK_1[L]}{1 + K_1[L]} \quad (1)$$

$$L_t = [L]\left(1 + \frac{ncK_1}{1 + K_1[L]}\right) \quad (2)$$

**Statistical Analyses.** Results are expressed as the means ± standard deviation (SD). One-way ANOVA was performed to test the effect of variation factors. If significant effects were found at a 95% confidence level ($p < 0.05$), then ANOVA was followed by a Tukey−Kramer HSD post hoc test to identify differences among groups (XLStat software, version 2008.3.02, Addinsoft SARL, Paris, France).

## RESULTS AND DISCUSSION

The present article first reports on our efforts to refine the chemical models of the gastric environment through a real integration of the physiological conditions prevailing in this compartment (*14*, *15*). The main forms of dietary lipids are triacylglycerols, which are readily emulsified in the stomach in the presence of amphiphilic food proteins and phospholipids following antral contractions. We thus designed 10% sunflower oil-in-water emulsions stabilized by either BSA or PL in order to investigate the influence of the interface composition on lipid oxidation. After the ingestion of vegetable purees, the stomach pH sharply increases to 5.4−6.2 in less than 30 min before slowly returning to a basal pH lower than 2 along gastric emptying (*22*). This study then focused on dietary iron-induced lipid oxidation and polyphenol stability in the early step of digestion (pH 5.8−6.0). The most redox-active heme form of dietary iron is metmyoglobin ($MbFe^{III}$), which accumulates after acid-catalyzed autoxidation of the Fe(II) state of meat myoglobin in postmortem processes. The level added to the emulsions corresponds to the consumption of 2 steaks (*23*).

**Characterization of the BSA and PL Model Emulsions.** The surface mean diameter of oil droplets $d_{32}$ was estimated to be 2.4 (±0.2) $\mu$m for the BSA-stabilized emulsions, whereas PL-stabilized ones exhibited a larger $d_{32}$ of 2.8 (±0.3) $\mu$m. Besides, the particle size distribution was in the physiological range (*6*, *22*) with a larger dispersion for the PL model (0.4−60 $\mu$m) compared to that for the BSA model (0.4−20 $\mu$m). During the course of lipid oxidation, $d_{32}$ increased only in the PL model as a possible result of the coalescence of lipid droplets.

**Lipid Oxidation in the Model Emulsions.** The accumulation of conjugated dienes (CD) as primary products of lipid oxidation was monitored by UV spectroscopy. At pH 5.8−6.0 and at 37 °C, metmyoglobin ($MbFe^{III}$) immediately triggered the oxidation of both BSA- and PL-stabilized emulsions, which suggests the presence of initial amounts of hydroperoxides essential to its activation (*24*). In our work, those lipid hydroperoxides could stem from the emulsion components: triacylglycerols, phospholipids, or even fatty acids typically contaminating BSA commercial samples. They could be present in the initial samples or mainly accumulated during the steps of homogenization and sonication. Since lipid hydroperoxides can actually form in lipid-containing foods during processing, storage, cooking, and possibly during digestion, their presence in our emulsions at the starting point of the oxidation process (addition of metmyoglobin) can be regarded as nutritionally relevant. In addition, the initial CD concentrations were estimated to be 0.9 mM and 1−1.5 mM for, respectively, BSA- and PL-stabilized emulsions (data not shown), which confirms that lipid oxidation prior to metmyoglobin addition is low.

In the BSA model, the peroxidation rate following metmyoglobin addition is 20-fold higher than that in the control experiment (4-fold in the PL model, **Figure 1**) It is thus quite clear that most of the CD are accumulated via metmyoglobin-induced peroxidation. However, it is not possible to distinguish among CD arising from triacylglycerols, phospholipids, or BSA-bound fatty acids. Given the huge excess of PUFA moieties in the triacylglycerol fraction (PUFA in oil/PUFA in PL ratio = 45 and PUFA in oil/PUFA in BSA ratio ≫ 500), most CD are likely to derive from the oil part of the emulsion even though interfacial lipids could be more rapidly oxidized because of a preferential access to pro-oxidant species in the aqueous phase. Anyway, lipid oxidation in the stomach may affect any type of lipids with similar

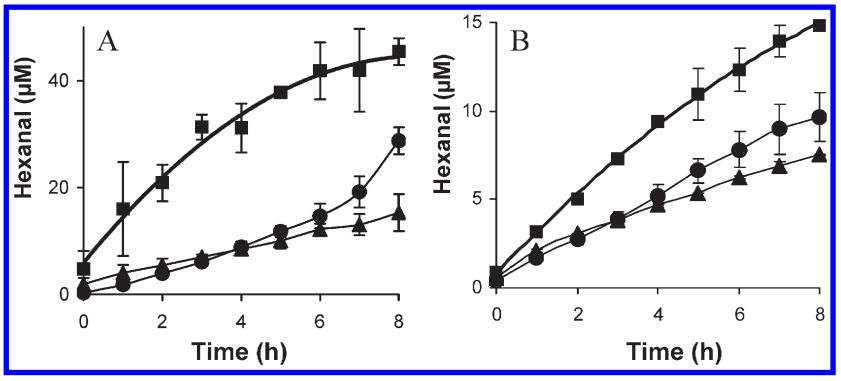


**Figure 2.** Formation of hexanal in the BSA model (**A**) and in the PL model (**B**) in the presence of metmyoglobin (20 $\mu$M), without quercetin (■) or with quercetin at 25 $\mu$M (●) and 100 $\mu$M (▲).

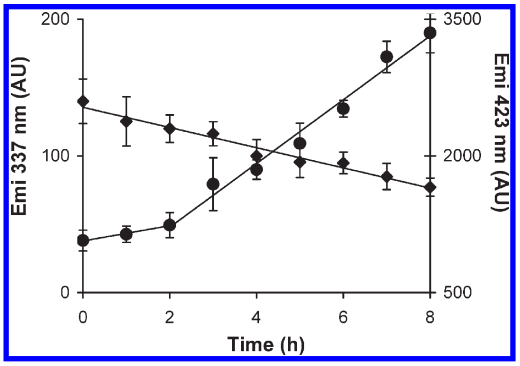


**Figure 3.** Front-face fluorescence emission of BSA-stabilized emulsions in $MbFe^{III}$-initiated oxidation. Monitoring of Trp at 337 nm (♦, excitation at 290 nm) and of new pigments at 423 nm (●, excitation at 360 nm).

deleterious consequences, and thus, a global approach such as CD monitoring may be considered pertinent.

In the $MbFe^{III}$-initiated lipid oxidation, CD accumulation was nearly linear, and the corresponding rates reached 3.8 mM CD/h ($R^2 = 0.985$) in the BSA model and 1.7 mM CD/h ($R^2 = 0.999$) in the PL model (**Figure 1**). The weak differences in oil−water interfacial areas, 2.3 $m^2$/g oil for the BSA model and 2.0 $m^2$/g for the PL model, can hardly explain the twice as fast oxidation rate within the BSA model. Other factors such as electrostatic interactions between the emulsifier and the oxidation initiator are known to favor lipid oxidation (ref *25* and refs therein). Indeed, at pH 6.0, BSA and $MbFe^{III}$ are, respectively, negatively and positively charged, and protein−protein interactions may help locate $MbFe^{III}$ at the interface leading to efficient initiation. Such stabilizing interactions cannot take place with the zwitterionic heads of phosphatidylcholine and phosphatidylethanolamine, the main phospholipids in the PL model. With an estimated BSA adsorption of 3 mg/$m^2$ of the interface (*26*), it can be calculated that only 5% of BSA is located at the interface in the BSA model. On the basis of a molecular surface of 50 $Å^2$ for the polar heads of the PL (*27*) and formation of PL monolayers at the oil−water interface, it can be estimated that only 3.8% of the PL is required for covering the oil droplets. This suggests that most PL molecules may be assembled as liposomes in the aqueous phase.

Conjugated dienes further decompose to secondary oxidation products, some of which being volatile compounds. In particular, hexanal, pentanal, 1-octen-3-ol, (*E*)-2-heptenal, and (*E*)-2-octenal were identified in the emulsion headspace by SPME-GC-MS and chosen as markers of secondary oxidation. Sampling of the volatile compounds in the headspace was used to trace their concentrations back in the emulsion phase. After 8 h, hexanal (46 $\mu$M) and (*E*)-2-heptenal (49 $\mu$M) were by far the main volatile compounds in the BSA-stabilized emulsions followed by 1-octen-3-ol (20 $\mu$M), (*E*)-2-octenal (8 $\mu$M), and pentanal (5 $\mu$M) (data not shown). As already observed with CDs, the formation of volatile compounds was 2 to 6 times faster in BSA-stabilized emulsions than in PL-stabilized emulsions as shown for hexanal (**Figure 2**). These 5 major volatiles all arise from the oxidation of $n - 6$ fatty acids (*25*), such as linoleic acid for sunflower oil. Additionally, hexanal and pentanal are formed by the specific decomposition of the 13-hydroperoxide of linoleic acid, while (*E*)-2-heptenal is produced from the 9-hydroperoxide (*28*). Accordingly, they represent good markers of secondary lipid oxidation, although their concentrations were found to be 3 orders of magnitude lower than the CD concentration after 8 h.

As the initial concentration in oxidizable linoleyl residues in the emulsions is ca. 220 mM and concentrations in conjugated dienes not decomposed after 8 h are 28 mM and 13 mM for the BSA and PL models, the minimal oxidation rates are evaluated to be 13 and 6%, respectively. These elevated values highlight the efficiency of the metmyoglobin-induced peroxidation of sunflower oil in gastric-like conditions.

**Structural Modifications of BSA.** Modifications of the BSA protein concomitant to lipid oxidation were investigated directly in the emulsions by front-face fluorescence spectroscopy. The intrinsic fluorescence of native BSA is mainly due to its two Trp residues: one is located at the protein surface (Trp134), while the other is deeply buried in subdomain IIA in close proximity to subdomain IIIA (Trp212). During lipid oxidation, the tryptophan fluorescence at 337 nm ($\lambda_{exc} = 290$ nm) decreased linearly, which suggests Trp oxidation and/or modifications of the Trp environment (e.g., exposure of Trp212 to a less hydrophobic environment and subsequent fluorescent quenching) (**Figure 3**). Concomitantly, the fluorescence emission at 423 nm ($\lambda_{exc} = 360$ nm) of the newly formed fluorophores rose progressively after a 2-h lag phase. These pigments were attributed to oxidized lipid−protein adducts. Schiff base formation results from the addition of the amino group of Lys residues onto the carbonyl group of aldehydes, while Michael addition leads to covalent coupling between the double bond of 2-alkenals and Lys or His residues (*20*, *25*). Moreover, highly oxidizing intermediates such as oxyl and peroxyl radicals issued from the decomposition of lipid hydroperoxides have also been implicated in BSA carbonylation and loss of Lys residues (*29*).

**Inhibition of Lipid Oxidation by Polyphenols.** The capacity to inhibit $MbFe^{III}$-initiated lipid oxidation was evaluated for different polyphenols selected for their large dietary abundance and encompassing the main polyphenol subclasses (**Figure 4**). The flavonol quercetin and its 3-diglycoside rutin, and the flavanol (+)-catechin as well as the hydroxycinnamic derivatives

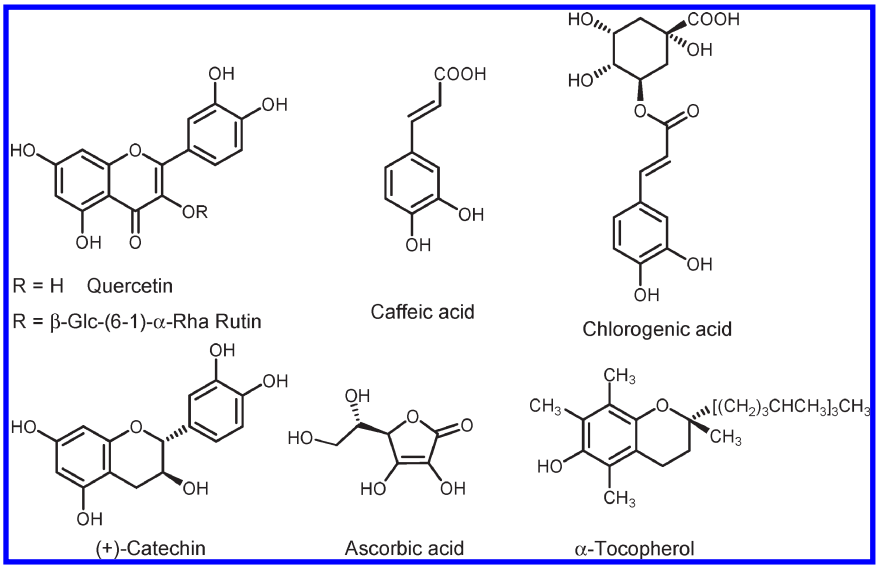


**Figure 4.** Chemical structures of the selected antioxidants.

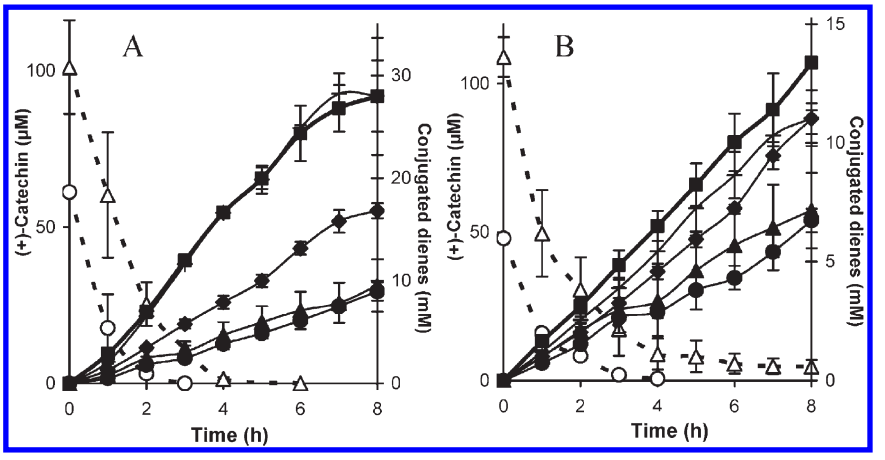


**Figure 5.** Inhibition by (+)-catechin of the accumulation of conjugated dienes in the BSA model (**A**) and in the PL model (**B**) in the presence of metmyoglobin (20 $\mu$M). (+)-Catechin concentrations: 0 (control, ■), 10 (+), 25 (♦), 50 (●), and 100 $\mu$M (▲). Concomitant oxidation of (+)-catechin at 50 $\mu$M (○) and 100 $\mu$M (△).

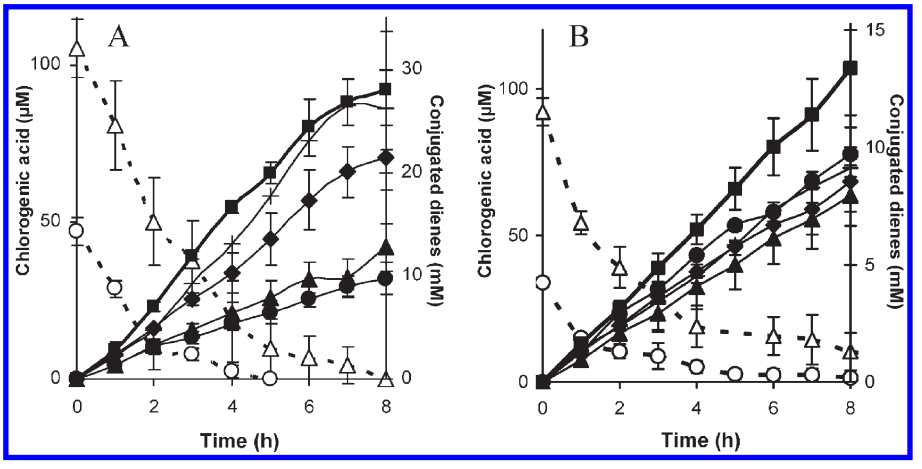


**Figure 6.** Inhibition by chlorogenic acid of the accumulation of conjugated dienes in the BSA model (**A**) and in the PL model (**B**) in the presence of metmyoglobin (20 $\mu$M). Chlorogenic acid concentrations: 0 (control, ■), 10 (+), 25 (♦), 50 (●), and 100 $\mu$M (▲). Concomitant oxidation of chlorogenic acid at 50 $\mu$M (○) and 100 $\mu$M (△).

caffeic acid and chlorogenic acid all afforded a significant protection to oxidizable lipids in BSA- and PL-stabilized emulsions (**Figures 1**, **5**, and **6**). The inhibition by polyphenols was concentration-dependent, although a saturation effect for concentrations above 50 $\mu$M was evidenced with catechin (**Figure 5**) caffeic acid, and chlorogenic acid (**Figure 6**). In the BSA model,

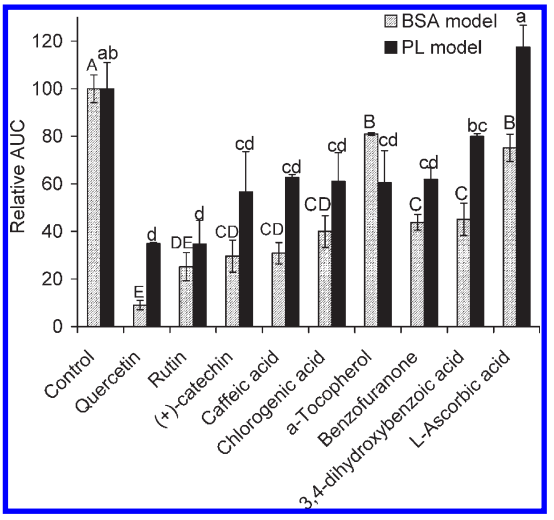


**Figure 7.** Inhibition of metmyoglobin-initiated lipid oxidation by various polyphenols in the BSA and PL models at pH 5.8−6.0. Polyphenol concentration = 100 $\mu$M. Same letters (capital letters for the BSA model and lowercase letters for the PL model) indicate no significant differences between the antioxidants ($p < 0.05$).

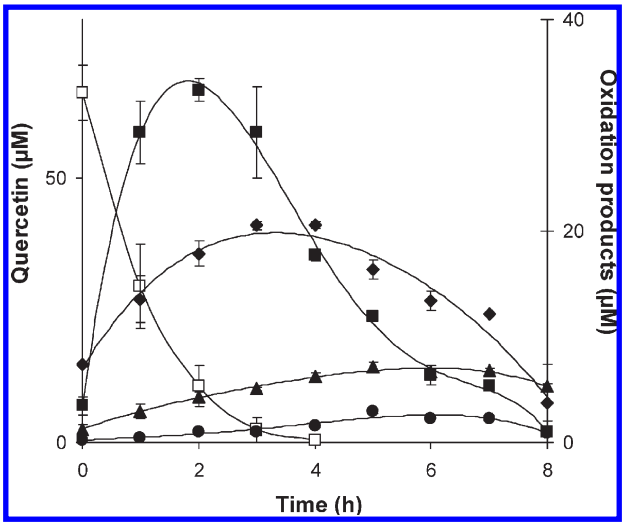


**Figure 8.** Consumption of quercetin 100 $\mu$M (□) and concomitant formation of quercetin oxidation products in the BSA model at pH 6.0: 3,4-dihydroxybenzoic acid (●), 1,3,5-trihydroxyphenylglyoxylic acid expressed as 3,4-dihydroxybenzoic acid equivalent (▲), the benzofuranone derivative (♦), and a quercetin dimer expressed as quercetin equivalent (■).

**Scheme 1.** Oxidation Pathway for Quercetin during the Inhibition of $MbFe^{III}$-Initiated Lipid Oxidation of BSA- and PL-Stabilized Emulsions

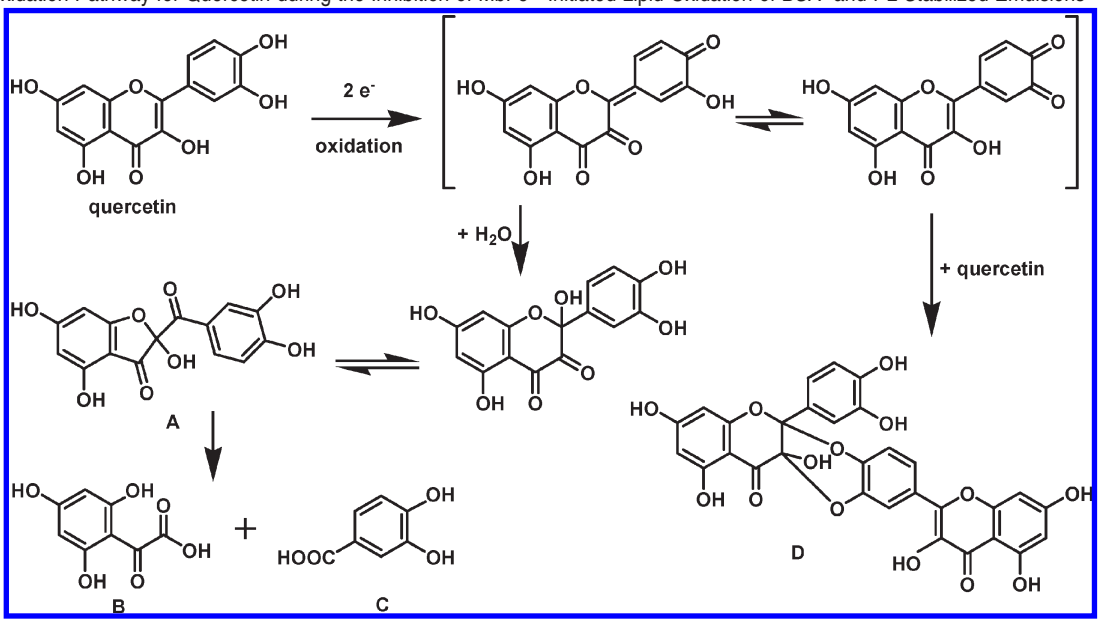


concentrations of quercetin (**Figure 1A**) and rutin (not shown) as low as 10 $\mu$M efficiently inhibited CD accumulation, whereas a minimal concentration of 25 $\mu$M was required for catechin, caffeic acid, and chlorogenic acid. Although inhibition patterns were slightly different in the PL model, low polyphenol concentrations proved to be as efficient if not more.

Noteworthy, in the BSA model, inhibition by quercetin resulted in pseudo lag phases (periods of very slow peroxidation) when the other polyphenols only depressed the CD accumulation rates (**Figures 1A**, **5A**, and **6A**). Indeed, pseudo lag phases of 3 and 4 h were exhibited for respective quercetin concentrations of 50 and 100 $\mu$M. Interestingly, the corresponding time periods required for complete consumption of quercetin were found to be 2 and 3 h. This suggests that some oxidation products of quercetin possess inhibitory properties.

In both models, the studied polyphenols efficiently inhibited the accumulation of conjugated dienes in the following order: quercetin ≥ rutin ≥ (+)-catechin ≈ caffeic acid ≈ chlorogenic acid (**Figure 7**). Inhibition rates higher than 60% were achieved for 100 $\mu$M concentrations in the BSA model, although these rates were closer to 40% in the PL model. Such a level corresponds to ca. 20−25 mg of bioaccessible polyphenols, which should be easily achieved during a meal assuming a mean polyphenol intake of 450−600 mg per day and per person as recently evaluated from a UK-focused database (*30*). The antioxidant capacities of the phenolic compounds were compared with those of the two antioxidant vitamins α-tocopherol and L-ascorbate. L-Ascorbate was a poor inhibitor of lipid oxidation in both model emulsions. The high sensitivity of L-ascorbate to autoxidation, with possible concomitant formation of hydrogen peroxide, could at least partly explain its inefficiency. α-Tocopherol could not be discriminated from polyphenols in the PL model, whereas it appears as a modest antioxidant in the BSA model, suggesting that it is rather bound to BSA as an inert complex.

The capacity of quercetin to inhibit the formation of volatile products was highly significant at concentrations of 25 and 100 $\mu$M in both models. Inhibition by 25 $\mu$M quercetin produced an extended pseudo lag phase of 6 h (**Figure 2**) consistent with the time required for cleavage of the CDs which started to accumulate after a 3−4 h period. In PL-stabilized emulsions, the inhibition of the volatile products also paralleled the inhibition of CD formation.

**Polyphenol Oxidation and Structural Elucidation of Oxidation Products.** In both emulsions, quercetin disappeared faster (3 h) followed by (+)-catechin (4 h), caffeic acid (6 h), chlorogenic acid (8 h), and rutin (> 8 h) (**Figures 1**, **5**, and **6**). A higher stability for the more hydrophilic conjugated forms (quinic ester and glycoside) can be noted.

As mentioned above, inhibition of lipid oxidation by quercetin in BSA-stabilized emulsions persisted well beyond the period required for the antioxidant consumption. This prompted us to further characterize the polyphenol oxidation products. For quercetin, HPLC-MS analysis revealed the formation of a more polar product with $m/z$ = 317 whose structure was assigned to 2-(3,4-dihydroxybenzoyl)-2,4,6-trihydroxy-3(2*H*)-benzofuranone (**A**) (**Scheme 1**). This oxidation product is formed by the addition of a water molecule onto the *p*-quinone methide intermediate resulting from two-electron oxidation of quercetin (*16*, *31*).

Smaller degradation products were identified as 2,4,6-trihydroxyphenylglyoxylic acid **B** ($m/z$ = 197) and 3,4-dihydroxybenzoic acid **C** ($m/z$ = 153), which respectively derive from the A- and B-rings of benzofuranone **A** after cleavage of its central ring (*30*). A dimer **D** ($m/z$ = 601) and a trimer of quercetin ($m/z$ = 902) were also identified in agreement with a previous report (*32*). The quercetin dimer **D** and benzofuranone **A** reached maximal concentrations at, respectively, 2 and 4 h (**Figure 8**), whereas 3,4-dihydroxybenzoic acid and 2,4,6-trihydroxyphenylglyoxylic acid accumulated more slowly along the consumption of the benzofuranone derivative.

The main degradation pathway for (+)-catechin was oligomerization as evidenced by the identification of two oxidized dimers ($m/z$ = 575, $\lambda_{max}$ = 420 and 386 nm). Colorless and colored dimers have already been produced through chemical and enzymatic oxidations (ref *33* and refs therein). Caffeic acid mainly yielded two dimers ($m/z$ = 357). Mass fragmentation revealed that one has an unbreakable C−C linkage, while the other has a breakable C−O linkage (fragment ion at $m/z$ = 179) (*34*). The slow oxidation of rutin and chlorogenic acid to minute amounts of new products did not provide sufficient sensitivity for structural elucidation.

**Antioxidant Activity of Quercetin Degradation Products.** Among quercetin oxidation products, the benzofuranone derivative **A**, 3,4-dihydroxybenzoic acid **C**, and dimer **D** retain the *o*-diphenolic structure (catechol nucleus) that is critical to the reducing capacity of polyphenols. Assessment of the antioxidant activity of **A** and **C** in the BSA and PL models at pH 5.8−6.0 revealed that they both rank among the efficient antioxidants tested in this work, although they are less potent than quercetin itself (**Figure 7**). The lower reducing capacity of benzofuranone **A** is linked to its higher redox potential of 0.69 V in aqueous acidic $CH_3CN$ versus 0.47 V for quercetin and can be ascribed to the loss of C-ring conjugation (*16*).

Degradation products possessing an *o*-diphenolic moiety may well contribute to the overall inhibitory capacity of the respective parent molecules. Similar observations have been reported for the inhibition of lipid oxidation in serum albumin−linoleic acid complexes (*31*).

**Binding Affinity of Quercetin and Rutin to BSA.** Quercetin and rutin, which have no fluorescence properties in their free state, display saturable emission intensities in the 490−590 nm range upon binding to BSA (excitation at 450 nm) (*21*). Binding constants $K$ and stoichiometry $n$ were first obtained using a Scatchard model. Since $n$ values close to 1 were found, $K$ values were reevaluated with the assumption of 1:1 binding. It was finally obtained: $K = 57\ (\pm 5) \times 10^3\ M^{-1}$ for quercetin and $K = 1.7\ (\pm 0.1) \times 10^3\ M^{-1}$ for rutin. This is in agreement with binding constants determined at pH 7.4 pointing to BSA having much lower affinities for rutin, caffeic acid, and chlorogenic acid ($K \approx 10^4\ M^{-1}$) than for quercetin ($K \approx 10^5\ M^{-1}$) (*21*, *35*−*37*). For concentrations in the 10−100 $\mu$M range, the percentage of BSA-bound quercetin can be calculated to be 87−92% versus only 23−25% for rutin. Although quercetin is mostly bound to BSA, its location at the interface is rather limited owing to the low adsorption of BSA (5%). Interestingly, works in our group have shown that BSA-bound quercetin was able to reduce ferrylmyoglobin ($MbFe^{IV}=O$), after the activation of $MbFe^{III}$ by $H_2O_2$, in a pH 5.8 buffer (manuscript submitted for publication). Either free or BSA-bound polyphenols can thus inhibit the initiation of lipid peroxidation.

In conclusion, model emulsions were designed to mimic the gastric environment found in the early phase of digestion after a meal including lipids, meat, and dietary polyphenols. They proved to be valuable tools to study the stability and efficiency of dietary antioxidants to inhibit heme-initiated lipid oxidation. The results in the two model emulsions are in agreement with those from Gorelik et al. who showed that heated red meat homogenized in a pH 3 human gastric fluid generated hydroperoxides and malondialdehyde, both reactions being inhibited by wine polyphenols (*13*). Because the antioxidant capacity of a meal is the result of a balance between its composition in dietary antioxidants, their ability to be released from the food matrix during digestion, and their interactions with endogenous components (enzymes and mucins), efforts will be devoted to take into account this complexity in our models so as to come closer to real gastric conditions.

## ACKNOWLEDGMENT

Michèle Viau is greatly acknowledged for helping with lipid analyses and Christian Giniès for helping with GC-MS analyses.

## LITERATURE CITED

(1) Hung, H. C.; Joshipura, K. J.; Jiang, R.; Hu, F. B.; Hunter, D.; Smith-Warner, S. A.; Colditz, G. A.; Rosner, B.; Spiegelman, D.; Willett, W. C. Fruit and vegetable intake and risk of major chronic disease. *J. Natl. Cancer Inst.* **2004**, *96*, 1577–1584.

(2) Arts, I. C. W.; Hollman, P. C. H. Polyphenols and disease risk in epidemiologic studies. *Am. J. Clin. Nutr.* **2005**, *81*, 317S–325S.

(3) Manach, C.; Scalbert, A.; Morand, C.; Remesy, C.; Jimenez, L. Polyphenols: food sources and bioavailability. *Am. J. Clin. Nutr.* **2004**, *79*, 727–747.

(4) Day, A. J.; Bao, Y.; Morgan, M. R. A.; Williamson, G. Conjugation position of quercetin glucuronides and effect on biological activity. *Free Radical Biol. Med.* **2000**, *29*, 1234–1243.

(5) Halliwell, B.; Zhao, K. C.; Whiteman, M. The gastrointestinal tract: A major site of antioxidant action? *Free Radical Res.* **2000**, *33*, 819–830.

(6) Armand, M.; Borel, P.; Dubois, C.; Senft, M.; Peyrot, J.; Salducci, J.; Lafont, H.; Lairon, D. Characterization of emulsions and lipolysis of dietary lipids in the human stomach. *Am. J. Physiol.* **1994**, *266*, G372–G381.

(7) Kanner, J.; Lapidot, T. The stomach as a bioreactor: dietary lipid peroxidation in the gastric fluid and the effects of plant-derived antioxidants. *Free Radical Biol. Med.* **2001**, *31*, 1388–1395.

(8) Kanazawa, K.; Ashida, H. Dietary hydroperoxides of linoleic acid decompose to aldehydes in stomach before being absorbed into the body. *Biochim. Biophys. Acta* **1998**, *1393*, 349–361.

(9) Kanner, J. Dietary advanced lipid oxidation end-products are risk factors to human health. *Mol. Nutr. Food Res.* **2007**, *51*, 1094–1101.
(10) Uchida, K. Role of reactive aldehydes in cardiovascular diseases. *Free Radical Biol. Med.* **2000**, *28*, 1685–1696.
(11) Staprans, I.; Rapp, J. H.; Pan, X.; Feingold, K. R. Oxidized lipids in the diet are incorporated by the liver into very low density lipoprotein in rats. *J. Lipid Res.* **1996**, *37*, 420–430.
(12) Ursini, F.; Sevanian, A. Postprandial oxidative stress. *Biol. Chem.* **2002**, *383*, 599–605.
(13) Gorelik, S.; Lapidot, T.; Shaham, I.; Granit, R.; Ligumsky, M.; Kohen, R.; Kanner, J. Lipid peroxidation and coupled vitamin oxidation in simulated and human gastric fluid inhibited by dietary polyphenols: health implications. *J. Agric. Food Chem.* **2005**, *53*, 3397–3402.
(14) Goupy, P.; Vulcain, E.; Caris-Veyrat, C. Dangles, O. Dietary antioxidants as inhibitors of the heme-induced peroxidation of linoleic acid: Mechanism of action and synergism. *Free Radical Biol. Med.* **2007**, *43*, 933–946.
(15) Vulcain, E.; Goupy, P.; Caris-Veyrat, C. Dangles, O. Inhibition of the metmyoglobin-induced peroxidation of linoleic acid by dietary antioxidants: action in the aqueous vs. lipid phase. *Free Radical Res.* **2005**, *39*, 547–563.
(16) Jungbluth, G.; Ruhling, I.; Ternes, W. Oxidation of flavonols with Cu(II), Fe(II) and Fe(III) in aqueous media. *J. Chem. Soc., Perkin Trans.* **2000**, *2*, 1946–1952.
(17) Villiere, A.; Viau, M.; Bronnec, I.; Moreau, N.; Genot, C. Oxidative stability of bovine serum albumin- and sodium caseinate-stabilized emulsions depends on metal availability. *J. Agric. Food Chem.* **2005**, *53*, 1514–1520.
(18) Mikkelsen, A.; Skibsted, L. H. Acid-catalysed reduction of ferrylmyoglobin: product distribution and kinetics of autoreduction and reduction by NADH. *Z. Lebensm.-Unters. Forsch.* **1995**, *200*, 171–177.
(19) Pryor, W. A.; Castle, L. Chemical Methods for the Detection of Lipid Hydroperoxydes. In *Oxygen Radicals in Biological Systems*; Packer, L., Ed.; Academic Press: Orlando, FL, 1984; pp 293−295.
(20) Rampon, V.; Lethuaut, L.; Mouhous-Riou, N.; Genot, C. Interface characterization and aging of bovine serum albumin stabilized oil-in-water emulsions as revealed by front-surface fluorescence. *J. Agric. Food Chem.* **2001**, *49*, 4046–4051.
(21) Dufour, C.; Dangles, O. Flavonoid-serum albumin complexation: determination of binding constants and binding sites by fluorescence spectroscopy. *Biochim. Biophys. Acta* **2005**, *1721*, 164–173.
(22) Tyssandier, V.; Reboul, E.; Dumas, J. F.; Bouteloup-Demange, C.; Armand, M.; Marcand, J.; Sallas, M.; Borel, P. Processing of vegetable-borne carotenoids in the human stomach and duodenum. *Am. J. Physiol.* **2003**, *284*, G913–G923.
(23) Dosi, R.; Maro, A. D.; Chambery, A.; Colonna, G.; Costantini, S.; Geraci, G.; Parente, A. Characterization and kinetics studies of water buffalo (Bubalus bubalis) myoglobin. *Comp. Biochem. Physiol., Part B: Biochem. Mol. Biol.* **2006**, *145*, 230–238.
(24) Baron, C. P.; Andersen, H. J. Myoglobin-induced lipid oxidation: a review. *J. Agric. Food Chem.* **2002**, *50*, 3887–3897.
(25) Genot, C.; Meynier, A.; Riaublanc, A. Lipid Oxidation in Emulsions. In *Lipid Oxidation Pathways*; Kamal-Eldin, A. Ed.; AOCS Press: Champaign, IL, 2003; pp 190−234.
(26) Kong, L. G.; Beattie, J. K.; Hunter, R. J. Electroacoustic study of BSA or lecithin stabilised soybean oil-in-water emulsions and SDS effect. *Colloids Surf., B* **2003**, *27*, 11–21.
(27) Pathirana, S.; Neely, W. C.; Vodyanoy, V. Condensing and expanding effects of the odorants (+)-and (-)-carvone on phospholipid monolayers. *Langmuir* **1998**, *14*, 679–682.
(28) Keszler, A.; Kriska, T.; Nemeth, A. Mechanism of volatile compound production during storage of sunflower oil. *J. Agric. Food Chem.* **2000**, *48*, 5981–5985.
(29) Refsgaard, H. H. F.; Tsai, L.; Stadtman, E. R. Modifications of proteins by polyunsaturated fatty acid peroxidation products. *Proc. Natl. Acad. Sci. U.S.A.* **2000**, *97*, 611–616.
(30) Clifford, M.; Brown, J. E. Dietary Flavonoids and Health: Broadening the Perspective. In *Flavonoids: Chemistry, Biochemistry and Applications*; Andersen, O., Markham, K., Eds; CRC Press: Boca Raton, FL, 2006; pp 319−370.
(31) Dufour, C.; Loonis, M. Flavonoids and their oxidation products protect efficiently albumin-bound linoleic acid in a model of plasma oxidation. *Biochim. Biophys. Acta* **2007**, *1770*, 958–965.
(32) Krishnamachari, V.; Levine, L. H.; Zhou, C.; Pare, P. W. In vitro flavon-3-ol oxidation mediated by a B ring hydroxylation pattern. *Chem. Res. Toxicol.* **2004**, *17*, 795–804.
(33) Dangles, O.; Fargeix, G.; Dufour, C. Antioxidant properties of anthocyanins and tannins: a mechanistic investigation with catechin and the 3′,4′,7-trihydroxyflavylium ion. *J. Chem. Soc., Perkin Trans.* **2000**, *2*, 1653–1663.
(34) Roche, M.; Dufour, C.; Mora, N.; Dangles, O. Antioxidant activity of olive phenols: mechanistic investigation and characterization of oxidation products by mass spectrometry. *Org. Biomol. Chem.* **2005**, *3*, 423–430.
(35) Adzet, T.; Camarasa, J.; Escubedo, E.; Merlos, M. In vitro study of caffeic acid - BSA interaction. *Eur. J. Drug Metab. Pharm.* **1988**, *13*, 11–14.
(36) Prigent, S. V. E.; Gruppen, H.; Visser, A.; van Koningsveld, G. A.; de Jong, G. A. H.; Voragen, A. G. J. Effects of non-covalent interactions with 5-O-caffeoylquinic acid (chlorogenic acid) on the heat denaturation and solubility of globular proteins. *J. Agric. Food Chem.* **2003**, *51*, 5088–5095.
(37) Rawel, H. A.; Meidtner, K.; Kroll, J. Binding of selected phenolic compounds to proteins. *J. Agric. Food Chem.* **2005**, *53*, 4228–4235.

**Received for review July 1, 2009. Revised manuscript received October 16, 2009. Accepted October 19, 2009. B.L. thanks the PACA Region and INRA for the financial support of a Ph.D. grant.**